RSC Advances

PAPER

View Article Online
View Journal | View Issue



Cite this: *RSC Adv.*, 2021, **11**, 30041

# Efficient artificial light-harvesting system constructed from supramolecular polymers with AIE property†

Tangxin Xiao, * Yong Shen, Cheng Bao, Kai Diao, Dongxing Ren, Hongwei Qian and Liangliang Zhang

Received 17th August 2021
Accepted 26th August 2021

DOI: 10.1039/d1ra06239e

rsc.li/rsc-advances

Supramolecular luminescent materials in water have attracted much interest due to their excellent tunability, multi-color emission, and environment-friendly behavior. However, hydrophobic chromophores are often affected by poor solubility and aggregation-caused quenching effects in aqueous media. Herein, we report a water-phase artificial light-harvesting system based on an AIE-type supramolecular polymer. Specifically, dispersed nanoparticles in water were prepared from an AIE chromophore-bridged ditopic ureidopyrimidinone (**M**) based supramolecular polymer with the assistance of surfactants. By co-assembling the hydrophobic chromophores **NDI** as energy acceptor into the nanocarriers, artificial light-harvesting systems (**M**–**NDI**) could be successfully constructed, exhibiting efficient energy transfer and high antenna effects. Furthermore, the spectral emission of the system could be continuously tuned with a relatively small number of acceptors. This work develops an efficient supramolecular light-harvesting system in water, which has potential applications in dynamic luminescent materials.



## Introduction

Solar energy harvesting and transfer are key points during the photosynthesis process.[1] The natural light-harvesting systems (LHSs) are complex supramolecular assemblies, in which large numbers of chromophores need to be densely stacked for high photosynthetic efficiency.[2] In artificial systems, scientists usually designed special scaffolds to accommodate chromophores to avoid aggregation-caused quenching (ACQ) and enhance Förster resonance energy transfer (FRET) between chromophores.[3] Such scaffolds are ranging from macrocycles,[4] DNA,[5] and cyclic peptides.[6] The introduction of aggregation-induced emission fluorogens (AIEgens) into this research field greatly simplifies the construction process of special scaffolds.[7] Specifically, the strategy of combining AIEgens and self-assembly, referred as supramolecular assembly-induced emission (SAIE), provides new motivations to develop new AIE materials.[8] Inspired by the above concept, a lot of AIE-type light-harvesting materials by mimicking photosynthesis have been fabricated for different applications, such as fluorescent probes,[9] luminescent materials,[10] bio-imaging,[11] and photocatalysis.[12]

Supramolecular polymers, driven by non-covalent interactions between monomeric building blocks, show outstanding reversibility, degradability, and stimuli-responsiveness, exhibiting broad potential applications in environmental and materials science.[13] Supramolecular polymerization is an excellent strategy for constructing LHSs, which not only can assemble chromophores together to pack tightly but also can enhance SAIE of the chromophores.[14] Among different types of non-covalent interactions, ureidopyrimidinone (UPy)-based quadruple hydrogen bonding (QHB) displays great potential on account of its strong binding constant and self-complementary.[15] In our previous studies, QHB has been used by us to construct various supramolecular polymers[16] and other supramolecular architectures.[17] In this work, we present the construction of a light-harvesting system by employing QHB supramolecular polymers with the AIE property.

The building block of the supramolecular polymer is a fixed tetraphenylethylene (FTPE)[18] group bridged ditopic UPy monomer (**M**), which also served as the energy donor (Fig. 1). Herein, the FTPE group endows **M** with SAIE behavior, while the UPy motif provides **M** with supramolecular polymerization capability *via* QHB. As a result, **M** can form AIE-type supramolecular polymers in organic solvents, such as chloroform or dichloromethane (DCM). Furthermore, the supramolecular polymer can be further self-assembled into water-dispersed NPs by using the mini-emulsion method based on the surfactant cetyltrimethyl ammonium bromide (CTAB). Moreover, by loading the synthesized dye **NDI** as energy acceptor to the NPs, an artificial LHS in

*School of Petrochemical Engineering, Changzhou University, Changzhou, 213164, China. E-mail: xiaotangxin@cczu.edu.cn*

† Electronic supplementary information (ESI) available: Experimental details, additional NMR spectra, and HR-ESI-MS spectra of individual compound. See DOI: 10.1039/d1ra06239e

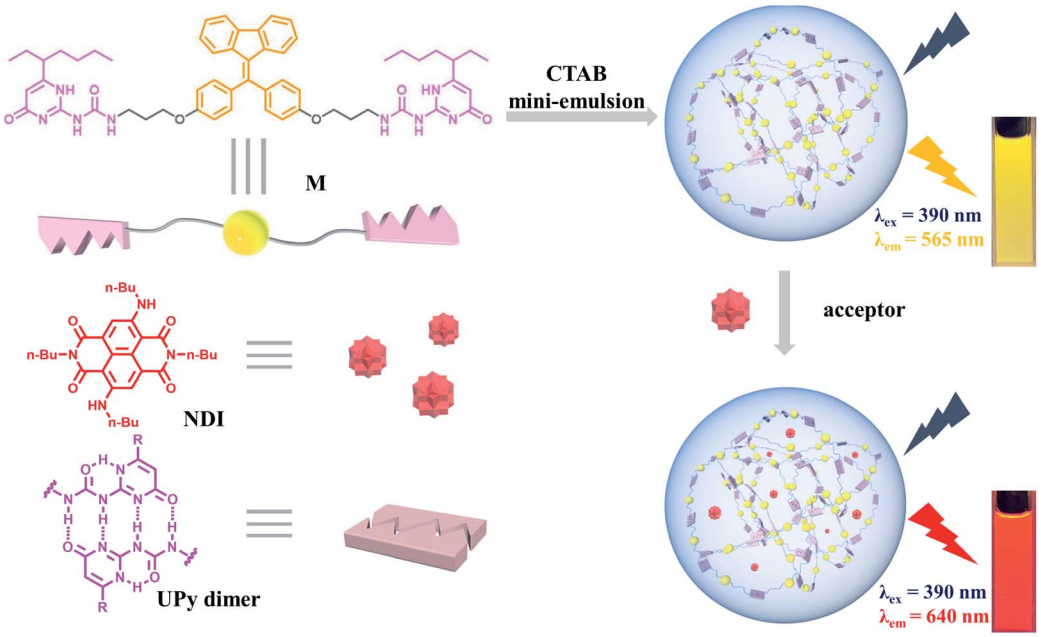


Fig. 1 Schematic illustration of the construction of light-harvesting NPs based on **M** and **NDI**.

aqueous media could be successfully fabricated. Due to the FRET process between **M** and **NDI**, the aqueous NPs were endowed with efficient light-harvesting capability and tunable emission. In our system, each component plays multiple roles to minimize the complexity of the system. For example, **M** is not only a supramolecular polymerization unit, but also a light harvesting antenna and energy donor. CTAB not only acts as a surfactant, but also mimics membrane lipids in natural photosynthesis. **NDI** has the dual-role of collecting energy from **M** and achieving long-wavelength emission simultaneously. Therefore, the **M–NDI** system appeared to be an interesting light-harvesting platform with great potentials in luminescent materials and bioimaging agents.

## Results and discussion

Monomer **M** can be obtained by condensation of **A** and **B** in dry $CHCl_3$ at room temperature (Scheme 1 and Fig. S7–S9, ESI†). Precursor **A** was synthesized according to our previous report,[19] while intermediate **B** was prepared according to literature report.[20] The association of **M** monomers through QHB was confirmed by $^1$H NMR. The characteristic N–H signals occurred in the down field region (between 10.0 and 14.0 ppm) indicates that the UPy units are dimerized by QHB (Fig. S7, ESI†). Through the logarithmic curve of specific viscosity *versus* monomer concentration, it can be found that the slope (2.02) has not changed (Fig. S1, ESI†), indicating that **M** can form a supramolecular polymer when the concentration is very low (<2 mM).

In order to study the AIE property of **M**, the fluorescence spectra of **M** in mixed hexane/DCM solutions were studied. It showed no emission when **M** was dissolved in the pure good solvent DCM (Fig. 2a). When increasing the poor solvent hexane to 92%, a moderate emission was shown. As hexane increased to 98%, the intensity of the spectrum shows an enhanced increase. By utilizing a mini-emulsion approach, we fabricated water-dispersed NPs from supramolecular polymer of **M**. 50 μL solution of **M** ([**M**] = 10 mM) in DCM was added to an aqueous

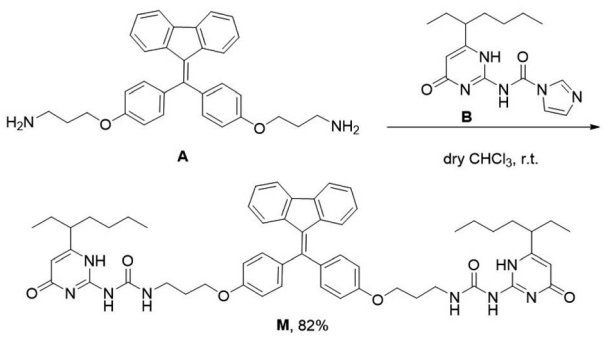


Scheme 1 Synthesis of **M**.

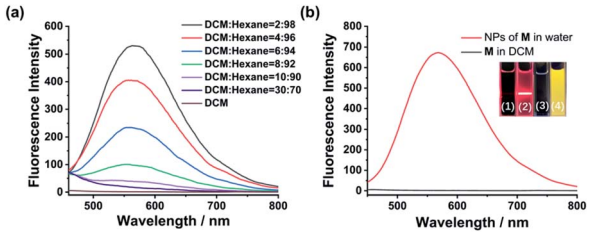


Fig. 2 (a) Fluorescence spectra of **M** *versus* hexane fraction in DCM/hexane mixtures. (b) Fluorescence spectra of molecule **M** in DCM and NPs of **M** in water upon excitation at 390 nm. Insets: the Tyndall effect of (1) **M** in DCM and (2) NPs of **M** in water; photographs of (3) **M** in DCM and (4) NPs of **M** in water under UV lamp irradiation. [**M**] = $5 \times 10^{-5}$ M.

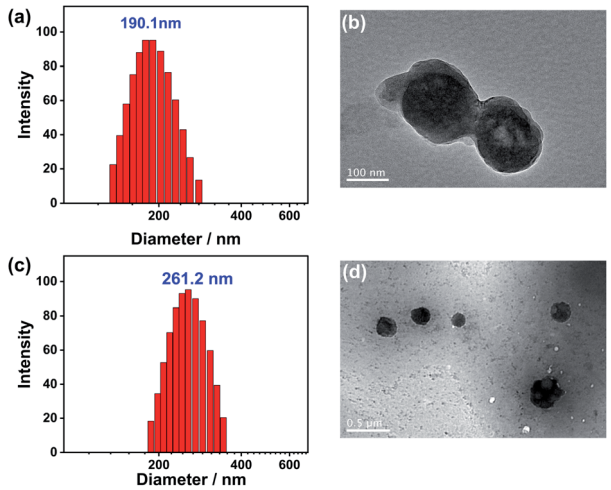


Fig. 3 DLS data of (a) NPs of **M** and (c) NPs of **M–NDI** in water at 25 °C. TEM images of (b) NPs of **M** and (d) NPs of **M–NDI** ([**M**] = $5 \times 10^{-5}$ M, [**NDI**] = $5 \times 10^{-7}$ M).

solution of CTAB (10 mL, [CTAB] = 1 mM), followed by ultrasonication for 30 min to produce the NPs. The obtained NPs solution of **M** ([**M**] = $5 \times 10^{-5}$ M) showed an obvious Tyndall effect, suggesting the existence of large number of nanoassemblies (Fig. 2b, inset (2)). By contrast, in the solution of **M** in DCM no Tyndall effect was observed, indicating that **M** was fully dissolved in the solvent (Fig. 2b, inset (1)). Moreover, the solution of **M** NPs displayed a bright yellow fluorescence under a UV lamp, suggesting that the SAIE behavior was occurring (Fig. 2b, inset (4)). The absolute fluorescence quantum yield of the sample was measured to be 2.91% (Fig. S3a, ESI†). On the contrary, the solution of **M** in DCM has no fluorescence under a UV irradiation (Fig. 2b, inset (3)). Meantime, the fluorescence measurements of **M** in different forms showed that there is no emission spectrum in DCM, but there is a strong emission spectrum in aqueous media (Fig. 2b). The strong emission of **M** NPs in water is owing to the restrict motion of FTPE group inside the NPs. These above results indicate that supramolecular polymeric NPs of **M** have been successfully constructed with the help of CTAB in water.

The size and morphology of the NPs were further characterized by dynamic light scattering (DLS) and transmission electron microscopy (TEM). DLS of the **M** NPs showed that they are well-defined nanoaggregates with the Z-average hydrodynamic diameter of 180–200 nm (Fig. 3a). The TEM image of the **M** NPs displayed a regular spherical morphology with diameters about 150 nm, good agreement with the DLS data (Fig. 3b). The hydrophobic micro-environment provided by CTAB and the entangled supramolecular polymers resulted in the efficient encapsulation of the acceptor molecules, which could be loaded into the NPs by mini-emulsifying them simultaneously with **M**. The morphology of the obtained **M–NDI** NPs was then also characterized by DLS and TEM (Fig. 3c and d). Compared with the **M** NPs, the **NDI**-loaded one also exhibit well-defined

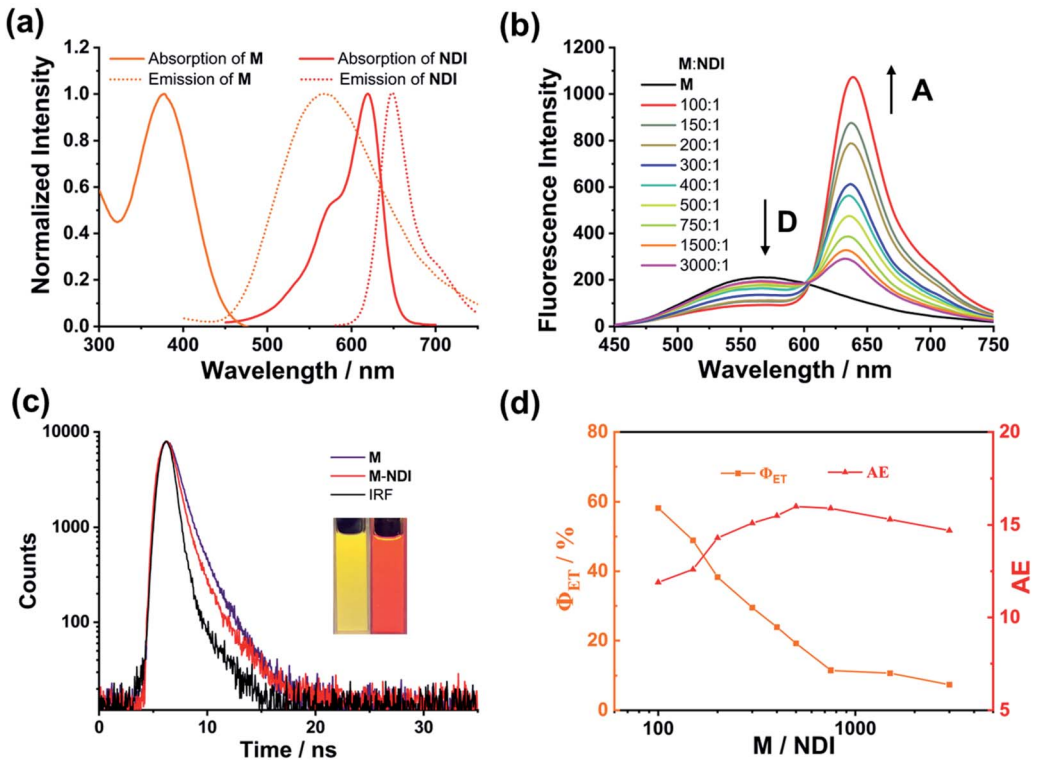


Fig. 4 (a) Normalized absorption spectra (solid line) and emission spectra (dashed line) of **M** and **NDI**, respectively. (b) Fluorescence spectra of NPs of **M** in water with different concentrations of **NDI**, [**M**] = $5 \times 10^{-5}$ M. (c) Fluorescence decay profiles of NPs of **M** and **M–NDI**, [**M**] = $5 \times 10^{-5}$ M, [**NDI**] = $5 \times 10^{-7}$ M. (d) Energy transfer efficiency ($\Phi_{ET}$) and antenna effect (AE) at different **M**/**NDI** ratios.

spherical shape, but are larger in size, which might be due to the hydrophobicity of the acceptor fluorophore.

The light-harvesting properties of the **NDI**-loaded NPs were further investigated. As shown in Fig. 4a, the absorption wavelength of **NDI** overlaps well with the emission peak of the **M** NPs, making the possibility of efficient FRET between the **M** (donor, D) and **NDI** (acceptor, A). Upon the addition of **NDI** to the NPs, when excited at 390 nm the fluorescence intensity of **M** at 565 nm dramatically decreased. Meantime, the emission peak of **NDI** at 640 nm continuously increased (Fig. 4b). Moreover, a remarkable change in fluorescence color from yellow to red was observed (Fig. 3c, inset). Furthermore, the absolute fluorescence quantum yield of **M–NDI** (A/D = 1%) exhibited a remarkable increase (13.35%, Fig. S3b, Table S2, ESI†), which might be because in this ratio **NDI** can harvest most of the excitation energy from **M** and subsequently emit as much as possible. To further confirm the occurrence of the energy-transfer process, time-resolved fluorescence spectroscopy was investigated. The fluorescence lifetime of the **M** NPs (Fig. 3c) was fitted as a double exponential decay, which showed $\tau_1$ = 1.61 ns and $\tau_2$ = 6.61 ns when monitored at 565 nm (Fig. S2, Table S1, ESI†). On the contrary, in the **M–NDI** system (A/D = 1%), the fluorescence lifetimes decreased to $\tau_1$ = 0.60 ns and $\tau_2$ = 4.87 ns respectively when monitored at 565 nm, indicating that the excitation energy was indeed transferred from the donor **M** to the acceptor **NDI** and that the **M–NDI** LHS had been successfully fabricated. In order to evaluate the capability of **M–NDI** LHS, both the energy-transfer efficiency ($\Phi_{ET}$) and the antenna effect (AE) were further investigated. Notably, $\Phi_{ET}$ represents the absorbed donor energy by the acceptor compared to the overall excitation energy of the donor; while AE is the amplification factor of the acceptor fluorescence when exciting the donor instead of directly exciting the acceptor. The $\Phi_{ET}$ of such system was 58.2% when co-assembling 1% **NDI** with **M** (Fig. S4 and Table S3, ESI†). Notably, the $\Phi_{ET}$ values gradually decreased with the decrease of **NDI** ratio (Fig. 4). Moreover, an AE value of 16.0-fold emission enhancement was observed when **M**/**NDI** = 500/1 (Fig. 4, Fig. S5, and Table S4, ESI†), indicating that the obtained **M–NDI** NPs can serve as an efficient LHS in aqueous media. We also carried out a control experiment. By employing the precursor **A** which bears FTPE core but without UPy group as antenna and energy donor (Fig. S6, ESI†), very poor energy transfer efficiencies and antenna effects for the system were observed, indicating that the quadruple hydrogen bonded supramolecular polymer are crucial for fabricating the LHSs.

The efficient **M–NDI** LHS creates a promising method to tune the fluorescence of the NPs in aqueous media. The system shows a ratio-dependent emission color change. As shown from the CIE 1931 chromaticity diagram (Fig. 5a), the NPs of **M** locates in the yellow area without the energy acceptor **NDI**. However, with the ratio of **NDI** increased from 3000 : 1 to 100 : 1, the fluorescence color of the LHS in water changed from yellow through orange to bright red gradually (Fig. 5b and c), indicating that an efficient energy transfer process had happened from the energy donor **M** to the energy acceptor **NDI**. It should be noting that this energy-transfer materials can be stored in water for a long time (1–2 weeks) without photobleaching. The reason for this is not only due to the efficient AIE property induced by FTPE group in **M**, but also because of the high fidelity of the QHB supramolecular polymers which was wrapped and stabilized by CTAB micelles.

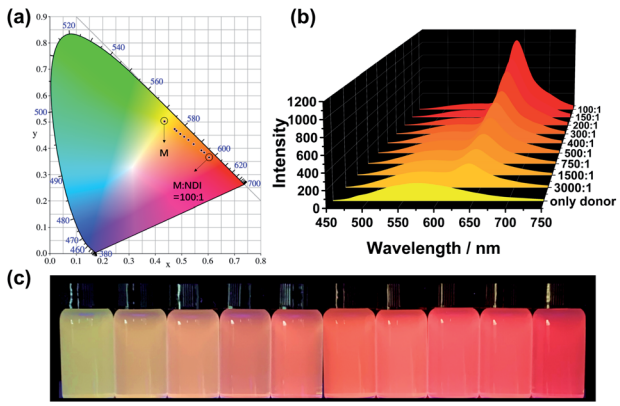


Fig. 5 (a) The CIE chromaticity diagram of photoluminescence color changes by varying the ratios of chromophores. (b) The fluorescence spectra of **M** in water with different concentrations of **NDI**. (c) Photographs of NPs in water with different **M–NDI** ratios. [**M**] = 5 × $10^{-5}$ M.

## Conclusions

In summary, we have fabricated an efficient artificial energy-transfer light-harvesting system in aqueous media based on supramolecular polymer. The supramolecular polymer was constructed by an FTPE group bridged ditopic UPy molecule **M** through quadruple hydrogen bonding. With the assistance of CTAB, the supramolecular polymers can further form stable nanoparticles in water by mini-emulsion method. By co-assembling hydrophobic fluorescent dye **NDI** simultaneously, an efficient artificial light-harvesting system **M–NDI** could be successfully constructed based on FRET process. By taking the advantages of SAIE, the ratio of donor and acceptor in nanoparticles could be easily controlled and the emission of the materials could be easily tuned with efficient energy-transfer and antenna effect. The composition of the system is relatively simple, and each module shows multi-functions, which provides the possibility for practical application. Therefore, the aqueous light-harvesting system developed here may have potential applications in dynamic luminescent materials and bio-imaging area.

## Conflicts of interest

There are no conflicts to declare.

## Acknowledgements

We gratefully thank the financial support from the National Natural Science Foundation of China (21702020).

## Notes and references

1 (*a*) D. I. Arnon, *Nature*, 1959, **184**, 10–21; (*b*) D. Gust and T. A. Moore, *Science*, 1989, **244**, 35–41; (*c*) N. S. Wigginton, *Science*, 2016, **352**, 1185–1186.

2 (*a*) S. Guo, Y. Song, Y. He, X. Y. Hu and L. Wang, *Angew. Chem., Int. Ed.*, 2018, **57**, 3163–3167; (*b*) J. J. Li, Y. Chen, J. Yu, N. Cheng and Y. Liu, *Adv. Mater.*, 2017, **29**, 1701905; (*c*) Z. Xu, S. Peng, Y. Y. Wang, J. K. Zhang, I. Lazar Alexandra and D. S. Guo, *Adv. Mater.*, 2016, **28**, 7666–7671.

3 (*a*) Y.-X. Hu, W.-J. Li, P.-P. Jia, X.-Q. Wang, L. Xu and H.-B. Yang, *Adv. Opt. Mater.,*, 2020, **8**, 2000265; (*b*) T. Xiao, W. Zhong, L. Zhou, L. Xu, X.-Q. Sun, R. B. P. Elmes, X.-Y. Hu and L. Wang, *Chin. Chem. Lett.*, 2019, **30**, 31–36.

4 (*a*) K. Acharyya, S. Bhattacharyya, H. Sepehrpour, S. Chakraborty, S. Lu, B. Shi, X. Li, P. S. Mukherjee and P. J. Stang, *J. Am. Chem. Soc.*, 2019, **141**, 14565–14569; (*b*) A. Sautter, B. K. Kaletaş, D. G. Schmid, R. Dobrawa, M. Zimine, G. Jung, I. H. M. van Stokkum, L. De Cola, R. M. Williams and F. Würthner, *J. Am. Chem. Soc.*, 2005, **127**, 6719–6729; (*c*) B. Valeur, E. Bardez, J.-M. Lehn, L. Jullien and J. Canceill, *Angew. Chem., Int. Ed.*, 1995, **33**, 2438–2439; (*d*) J. Pruchyathamkorn, W. J. Kendrick, A. T. Frawley, A. Mattioni, F. Caycedo-Soler, S. F. Huelga, M. B. Plenio and H. L. Anderson, *Angew. Chem., Int. Ed.*, 2020, **59**, 16455–16458.

5 (*a*) P. Ensslen and H.-A. Wagenknecht, *Acc. Chem. Res.*, 2015, **48**, 2724–2733; (*b*) P. K. Dutta, R. Varghese, J. Nangreave, S. Lin, H. Yan and Y. Liu, *J. Am. Chem. Soc.*, 2011, **133**, 11985–11993.

6 (*a*) Q. Song, S. Goia, J. Yang, S. C. L. Hall, M. Staniforth, V. G. Stavros and S. Perrier, *J. Am. Chem. Soc.*, 2021, **143**, 382–389; (*b*) T. Wang, X. Fan, J. Xu, R. Li, X. Yan, S. Liu, X. Jiang, F. Li and J. Liu, *ACS Macro Lett.*, 2019, **8**, 1128–1132.

7 (*a*) Y. Hong, J. W. Y. Lam and B. Z. Tang, *Chem. Soc. Rev.*, 2011, **40**, 5361–5388; (*b*) M. Cheng, C. Qian, Y. Ding, Y. Chen, T. Xiao, X. Lu, J. Jiang and L. Wang, *ACS Macro Lett.*, 2020, **2**, 425–429; (*c*) F. Würthner, *Angew. Chem., Int. Ed.*, 2020, **59**, 14192–14196.

8 (*a*) N. Song, D. X. Chen, M. C. Xia, X. L. Qiu, K. Ma, B. Xu, W. Tian and Y. W. Yang, *Chem. Commun.*, 2015, **51**, 5526–5529; (*b*) H. Wu and T. Xiao, *Front. Chem.*, 2020, **8**, 610093; (*c*) T. Xiao, L. Zhang, H. Wu, H. Qian, D. Ren, Z.-Y. Li and X.-Q. Sun, *Chem. Commun.*, 2021, **57**, 5782–5785; (*d*) X. Z. Yan, T. R. Cook, P. Wang, F. H. Huang and P. J. Stang, *Nat. Chem.*, 2015, **7**, 342–348.

9 (*a*) Z. Liu, X. Sun, X. Dai, J. Li, P. Li and Y. Liu, *J. Mater. Chem. C*, 2021, **9**, 1958–1965; (*b*) M. Su, Y.-N. Jing, H. Bao and W.-M. Wan, *Mater. Chem. Front.*, 2020, **4**, 2435–2442; (*c*) L. Ji, Y. Sang, G. Ouyang, D. Yang, P. Duan, Y. Jiang and M. Liu, *Angew. Chem., Int. Ed.*, 2019, **58**, 844–848.

10 (*a*) D. Li, J. Wang and X. Ma, *Adv. Opt. Mater.*, 2018, **6**, 1800273; (*b*) Y. Li, Y. Dong, L. Cheng, C. Qin, H. Nian, H. Zhang, Y. Yu and L. Cao, *J. Am. Chem. Soc.*, 2019, **141**, 8412–8415; (*c*) H.-Q. Peng, C.-L. Sun, L.-Y. Niu, Y.-Z. Chen, L.-Z. Wu, C.-H. Tung and Q.-Z. Yang, *Adv. Funct. Mater.*, 2016, **26**, 5483–5489; (*d*) Q. Wang, Q. Zhang, Q.-W. Zhang, X. Li, C.-X. Zhao, T.-Y. Xu, D.-H. Qu and H. Tian, *Nat. Commun.*, 2020, **11**, 158; (*e*) X.-H. Wang, N. Song, W. Hou, C.-Y. Wang, Y. Wang, J. Tang and Y.-W. Yang, *Adv. Mater.*, 2019, **31**, 1903962; (*f*) T. Xiao, X. Wei, H. Wu, K. Diao, Z.-Y. Li and X.-Q. Sun, *Dyes Pigm.*, 2021, **188**, 109161.

11 X. M. Chen, Q. Cao, H. K. Bisoyi, M. Wang, H. Yang and Q. Li, *Angew. Chem., Int. Ed.*, 2020, **59**, 10493–10497.

12 (*a*) D. Zhang, W. Yu, S. Li, Y. Xia, X. Li, Y. Li and T. Yi, *J. Am. Chem. Soc.*, 2021, **143**, 1313–1317; (*b*) X. Li, Y. Wang, A. Song, M. Zhang, M. Chen, M. Jiang, S. Yu, R. Wang and L. Xing, *Chin. J. Chem.*, 2021, **39**, DOI: 10.1002/cjoc.202100293; (*c*) W. J. Li, X. Q. Wang, D. Y. Zhang, Y. X. Hu, W. T. Xu, L. Xu, W. Wang and H. B. Yang, *Angew. Chem., Int. Ed.*, 2021, **60**, 18761–18768; (*d*) M. Hao, G. Sun, M. Zuo, Z. Xu, Y. Chen, X. Y. Hu and L. Wang, *Angew. Chem., Int. Ed.*, 2020, **59**, 10095–10100; (*e*) Z. Zhang, Z. Zhao, Y. Hou, H. Wang, X. Li, G. He and M. Zhang, *Angew. Chem., Int. Ed.*, 2019, **58**, 8862–8866.

13 (*a*) T. Aida, E. W. Meijer and S. I. Stupp, *Science*, 2012, **335**, 813–817; (*b*) L. Yang, X. Tan, Z. Wang and X. Zhang, *Chem. Rev.*, 2015, **115**, 7196–7239; (*c*) E. Krieg, M. M. C. Bastings, P. Besenius and B. Rybtchinski, *Chem. Rev.*, 2016, **116**, 2414–2477; (*d*) T. Xiao, L. Zhou, X.-Q. Sun, F. Huang, C. Lin and L. Wang, *Chin. Chem. Lett.*, 2020, **31**, 1–9.

14 (*a*) D. Dai, Z. Li, J. Yang, C. Wang, J. R. Wu, Y. Wang, D. Zhang and Y. W. Yang, *J. Am. Chem. Soc.*, 2019, **141**, 4756–4763; (*b*) P. Wang, X. Miao, Y. Meng, Q. Wang, J. Wang, H. Duan, Y. Li, C. Li, J. Liu and L. Cao, *ACS Appl. Mater. Interfaces*, 2020, **12**, 22630–22639; (*c*) T. Xiao, H. Wu, G. Sun, K. Diao, X. Wei, Z.-Y. Li, X.-Q. Sun and L. Wang, *Chem. Commun.*, 2020, **56**, 12021–12024.

15 R. P. Sijbesma, F. H. Beijer, L. Brunsveld, B. J. B. Folmer, J. H. K. K. Hirschberg, R. F. M. Lange, J. K. L. Lowe and E. W. Meijer, *Science*, 1997, **278**, 1601–1604.

16 (*a*) L. Qi, Y. Ding, T. Xiao, H. Wu, K. Diao, C. Bao, Y. Shen, Z. Li, X. Sun and L. Wang, *Chin. J. Org. Chem.*, 2020, **40**, 3847; (*b*) T. Xiao, W. Zhong, L. Qi, J. Gu, X. Feng, Y. Yin, Z.-Y. Li, X.-Q. Sun, M. Cheng and L. Wang, *Polym. Chem.*, 2019, **10**, 3342–3350; (*c*) T. Xiao, L. Xu, J. Götz, M. Cheng, F. Würthner, J. Gu, X. Feng, Z.-Y. Li, X.-Q. Sun and L. Wang, *Mater. Chem. Front.*, 2019, **3**, 2738–2745.

17 (*a*) T. Xiao, W. Zhong, W. Yang, L. Qi, Y. Gao, A. C. H. Sue, Z.-Y. Li, X.-Q. Sun, C. Lin and L. Wang, *Chem. Commun.*, 2020, **56**, 14385–14388; (*b*) T. Xiao, L. Xu, J. Wang, Z.-Y. Li, X.-Q. Sun and L. Wang, *Org. Chem. Front.*, 2019, **6**, 936–941.

18 (*a*) X. Gu, J. Yao, G. Zhang, Y. Yan, C. Zhang, Q. Peng, Q. Liao, Y. Wu, Z. Xu, Y. Zhao, H. Fu and D. Zhang, *Adv. Funct. Mater.*, 2012, **22**, 4862–4872; (*b*) J.-H. Wang, H.-T. Feng, J. Luo and Y.-S. Zheng, *J. Org. Chem.*, 2014, **79**, 5746–5751; (*c*) T. Xiao, L. Zhou, X. Wei, Z. Li and X. Sun, *Chin. J. Org. Chem.*, 2020, **40**, 944–949.

19 T. Xiao, J. Wang, Y. Shen, C. Bao, Z.-Y. Li, X.-Q. Sun and L. Wang, *Chin. Chem. Lett.*, 2021, **32**, 1377–1380.

20 H. M. Keizer, R. P. Sijbesma and E. W. Meijer, *Eur. J. Org. Chem.*, 2004, **2004**, 2553–2555.